UCLA

Title

Chemotherapy-Induced Inflammatory Gene Signature and Protumorigenic Phenotype in Pancreatic CAFs via Stress-Associated MAPK

Authors

Toste, Paul A
Nguyen, Andrew H
Kadera, Brian E
et al.

Chemotherapy-induced Inflammatory Gene Signature and Pro-tumorigenic Phenotype in Pancreatic CAFs via Stress-associated MAPK

Paul A. Toste[1], **Andrew H. Nguyen**[1], **Brian E. Kadera**[1], **Mindy Duong**[1], **Nanping Wu**[1], **Irmina Gawlas**[1], **Linh M. Tran**[2], **Mihir Bikhchandani**[1], **Luyi Li**[1], **Sanjeet G. Patel**[1], **David W. Dawson**[3,4], and **Timothy R. Donahue**[1,2,4,*]

[1]Department of Surgery, Division of General Surgery, David Geffen School of Medicine at University of California Los Angeles (UCLA), Los Angeles, CA, USA

[2]Department of Molecular and Medical Pharmacology, David Geffen School of Medicine at University of California Los Angeles (UCLA), Los Angeles, CA, USA

[3]Department of Pathology and Laboratory Medicine, David Geffen School of Medicine at University of California Los Angeles (UCLA), Los Angeles, CA, USA

[4]Jonsson Comprehensive Cancer Center, David Geffen School of Medicine at University of California Los Angeles (UCLA), Los Angeles, CA, USA

Abstract

Pancreatic ductal adenocarcinoma (PDAC) has a characteristically dense stroma comprised predominantly of cancer associated fibroblasts (CAFs). CAFs promote tumor growth, metastasis and treatment resistance. This study aimed to investigate the molecular changes and functional consequences associated with chemotherapy treatment of PDAC CAFs. Chemoresistant immortalized CAFs (R-CAFs) were generated by continuous incubation in gemcitabine. Gene expression differences between treatment naïve CAFs (N-CAFs) and R-CAFs were compared by array analysis. Functionally, tumor cells (TCs) were exposed to N-CAF or R-CAF conditioned media and assayed for migration, invasion and viability *in vitro*. Furthermore, a co-injection (TC and CAF) model was used to compare tumor growth *in vivo*. R-CAFs increased TC viability, migration and invasion compared to N-CAFs. *In vivo*, TCs co-injected with R-CAFs grew larger than those accompanied by N-CAFs. Genomic analysis demonstrated that R-CAFs had increased expression of various inflammatory mediators, similar to the previously described senescence-associated secretory phenotype (SASP). In addition, SASP mediators were found to be

*Corresponding author: Department of Surgery, 72-215 Center for the Health Sciences, 10833 LeConte Avenue, Los Angeles, CA 90095-6904, Phone: 310-206-7440, Fax: 310-206-2472, tdonahue@mednet.ucla.edu.

Conflicts of interest: None

upregulated in response to short duration treatment with gemcitabine in both immortalized and primary CAFs. Inhibition of stress-associated MAPK signaling (P38 MAPK or JNK) attenuated SASP induction as well as the tumor-supportive functions of chemotherapy-treated CAFs *in vitro* and *in vivo*. These results identify a negative consequence of chemotherapy on the PDAC microenvironment that could be targeted to improve the efficacy of current therapeutic regimens.

Keywords

Pancreatic cancer; cancer-associated fibroblast; SASP; P38 MAPK; JNK

Introduction

Pancreatic ductal adenocarcinoma (PDAC) is the fourth leading cause of cancer-related deaths in the United States. As a result of both late diagnosis and frequent resistance to chemotherapy, the overall 5-year survival rate of PDAC patients is 6% (1). Unfortunately, this dismal prognosis has remained essentially unchanged for several decades (2). Elucidating the molecular mechanisms that result in the characteristically poor response to treatment in PDAC will be essential to improving therapeutic responses.

A defining feature of PDAC is its dense tumor-associated stroma. The characteristic desmoplastic reaction is comprised of extracellular matrix along with several cell types including fibroblasts, leukocytes and endothelial cells (3). Cancer-associated fibroblasts (CAFs) are the predominant cell type in the tumor-associated stroma and function to support tumor development, growth and dissemination in a variety of ways (3-5). CAFs enhance tumor cell (TC) fitness by promoting proliferation (6,7), migration and invasion (6,8), immune evasion (9-11), and resistance to chemotherapy (12,13) as well as radiation (14). Because of their myriad tumor supportive functions, CAF-directed therapy is an emerging treatment strategy in PDAC (15,16).

CAFs contribute to chemoresistance via multiple mechanisms. The dense extracellular matrix synthesized by CAFs can act as a physical barrier to drug delivery (12,17,18). Additionally, CAFs create a microenvironmental niche that supports TC proliferation, resists apoptosis (6,19), and promotes cancer stem cell maintenance (20,21). Despite these well described roles in promoting chemoresistance, to our knowledge, the molecular consequences of chemotherapy treatment on PDAC CAFs have not been reported. There is evidence in prostate (22) and breast cancer (23) to suggest that chemotherapy can induce tumor-supportive molecular changes in CAFs. Understanding the consequences of chemotherapy treatment on PDAC CAFs could provide new insight into the limitations of current treatments and identify novel therapeutic targets.

In the present study we investigate the functional consequences as well as molecular changes associated with chemotherapy treatment of PDAC CAFs. We show that exposure of PDAC CAFs to cytotoxic chemotherapy results in increased tumor supportiveness mediated by the upregulation of multiple inflammatory cytokines.

Materials and Methods

Cell culture and treatments

Immortalized human PDAC CAFs were obtained from the lab of Dr. Rosa Wang (7). TC lines (MiaPaCa-2 and PANC-1) and immortalized CAFs were grown in DMEM supplemented with 10% FBS (Gemini) +1x penicillin-streptomycin (Invitrogen). Primary human CAFs were isolated from surgical pancreatic cancer specimens by the outgrowth method (24) and grown in DMEM/F12 + Glutamax (Invitrogen) supplemented with 10% FBS + 1x penicillin-streptomycin. Primary CAF isolation was conducted under an institutional review board approved protocol. Primary CAFs were characterized by wild type KRAS status and α-smooth muscle actin positivity as previously described (25).

Chemoresistant immortalized CAFs (R-CAFs) were generated by continuous incubation in media supplemented with 100nM gemcitabine (Sagent) for 4 weeks. A dose of 100nM gemcitabine was chosen because this is approximately the IC_{50} of these cells. Chemotherapy naïve immortalized CAFs (N-CAFs) were cultured alongside R-CAFs during their 4 week incubation to avoid any differences that could result from passaging. After the 4 week incubation, cells were passaged in media containing 100nM gemcitabine. R-CAFs were subjected to no more than 8 passages in gemcitabine containing media, and N-CAFs were treated the same in standard media. R-CAFs were compared to N-CAFs as described. R-CAFs were confirmed to be resistant to various doses of gemcitabine by MTT assay (Supplementary Fig. S1).

The following drugs were suspended in DMSO: SB203580, NVP-BEZ235, KU-55933 (LC Laboratories); SP600125 (Tocris); VE-821 and AZD7762 (Selleckchem). Gemcitabine was suspended in PBS. Drug stocks were kept at −20°C, and drug containing media at given concentrations was made fresh for each experiment. DMSO as a vehicle control was used where appropriate.

Conditioned Media (CM)

N-CAFs and R-CAFs were plated in 10cm plates and grown to confluence in standard media. Once confluent, cells were washed with PBS three times and placed in 10ml serum free DMEM. After 72h, conditioned media (CM) was harvested, centrifuged twice at 750g, and frozen in aliquots at −80°C. For short-term treatment, N-CAFs were plated in 10cm plates and treated with or without gemcitabine plus SB203580, SP600125 or DMSO control for 48h in serum containing media. Media was then changed to serum free without drugs for 24h and harvested and processed as above. For all experiments utilizing CM, it was thawed immediately prior to use and never re-frozen.

In vitro viability

Viability was measured by MTT assay. 4×10^5 cells were seeded into 96-well plates in 100μl CM supplemented with 1% FBS. At the desired time points, 10μl of 5mg/ml MTT (Molecular Probes) was added to each well and incubated for 4h at 37°C. Cells were then lysed with 100ul 10% SDS, 0.01M HCl and incubated overnight at 37°C. Absorbance readings were measured with a microplate reader at 560nm wavelength. All experiments

were performed in biologic triplicate and repeated at least twice. Data shown is from one representative experiment.

TC migration and invasion assays

TCs were incubated overnight in DMEM with 0.1% FBS followed by seeding 1×10^5 cells/well in 24-well cell culture inserts with PET membranes and 8μm pores (Corning). Cells were seeded in CM with 0.1% FBS, and CM with 10% FBS was placed in the bottom well. For migration assays, uncoated inserts were used, and TCs were allowed to migrate for 18h. For invasion assays, Matrigel-coated inserts were used, and TCs were allowed to invade for 28h. After completion of migration or invasion, cells on the lower surface of the membrane were fixed with 4% paraformaldehyde followed by 100% methanol for 10 min. each then stained with hematoxylin. Cell number in 5, 20X fields was determined for each insert. All experiments were performed in biologic triplicate and repeated at least twice. Data shown is from one representative experiment.

Xenograft model

1×10^5 MiaPaCa-2 or PANC-1 cells were subcutaneously implanted in the bilateral flanks of NOD/SCID/IL2γ knockout (NSG) mice along with 3×10^5 CAFs (N-CAF or R-CAF). 3×10^5 CAFs were injected intra-tumorally once a week thereafter. For experiments involving pre-treatment of cells, N-CAFs were treated for 48h prior to implantation with or the indicated drug concentrations. Tumors were measured weekly, and mice were sacrificed when tumor diameter approached 1cm. Repeat CAF injections were performed because of the observation that injected CAFs do not persist long-term in this tumor model (Supplementary Fig. S2). The formula π/6*L*W*H was used to calculate tumor volume. For all *in vivo* experiments, 6 mice were used for each condition.

Gene expression microarray

Total RNA was isolated from N-CAFs and R-CAFs using the miRNeasy mini kit (Qiagen). Gene expression array was performed in duplicate at the UCLA Clinical Microarray Core utilizing Affymetrix GeneChip Instrument Systems equipment (Affymetrix U133 Plus 2.0). RMA normalization was performed using Partek Genomics Suite software. Fold changes of 2 or -2 were used to identify differentially expressed genes. Study data are deposited in NCBI GEO under accession number GSE78982.

For pathway analysis, Fisher's exact test was used to screen pathways and gene sets in the Molecular Signatures Database v5.1 (http://www.broadinstitute.org/gsea/msigdb/index.jsp) that were significantly differentially expressed between R- and N-CAFs. A Fisher criterion of 2 was used to identify differently expressed genes. Fisher's exact test p-values were adjusted for multiple testing using the Benjamini and Hochberg approach. Gene set enrichment analysis (GSEA) for SASP genes was then performed on the gene sets identified to be significantly enriched (p 0.05) by the above described analysis. A previously described set of SASP genes was used: Table 1, Freund et al (26). Of note analysis was applied to those genes listed in Table 1 (26) encoding well-described inflammatory proteins, indicated by a plus sign. Fold change in $\log_2$ scale was used as a metric for ranking gene sets in the analysis.

qRT-PCR

Total RNA was isolated from cells using the Quick-RNA MiniPrep kit (Zymo). Reverse transcription was performed using the High Capacity cDNA Reverse Transcription kit (Applied Biosystems). Quantitative PCR was performed using EvaGreen qPCR Master Mix (Lamda Biotech). All PCR results were analyzed using the method reported by Livak et al (27). RPL13A was used as a housekeeper. Primers used are reported in Supplementary Table S1. All experiments were performed in technical triplicate and repeated at least twice. Data shown is the composite of two experiments.

Antibody-based cytokine array and ELISA

Full strength CM from N-CAFs or R-CAFs was assayed using the Human Cytokine Array Panel A (R&D Systems) according to manufacturer's instructions. Membranes were developed using standard chemiluminescent techniques. Pixel density was calculated using ImageLab software (Bio-Rad). ELISA for IL-8 was performed using full strength CM and the Human IL-8 ELISA Ready-Set-Go kit (eBioscience).

Western blots

Whole cell lysates were obtained using RIPA buffer. Proteins were separated on 10% SDS-PAGE gels at 100V for 3h and blotted to PVDF membranes at 25V overnight in 10% methanol containing transfer buffer. Primary antibodies were incubated overnight at 4°C and secondary antibodies were incubated for 1h at room temperature. Primary antibodies used were obtained from Cell Signaling: p-P38 1:1000 (#4511, Thr180/Tyr182), P38 1:1000 (#9212), p-JNK 1:1000 (#4668, Thr183/Tyr185), JNK 1:1000 (#9258), p-HSP27 1:500 (#2401, Ser82), HSP27 1:1000 (#2402), p-cJUN 1:1000 (#2361, Ser63), cJUN 1:1000 (#9165), p-Chk1 1:1000 (#2348, Ser345), Chk1 1:1000 (#2360), p-Chk2 1:1000 (#2661, Thr68), Chk2 1:1000 (#3440) and GeneTex: GAPDH 1:5000 (GTX627408). Chemiluminescent imaging was performed by incubation with anti-mouse- 1:10,000 or anti-rabbit- 1:5,000 HRP-conjugated secondary antibody (Jackson Labs) and SuperSignal West Pico or Femto (Thermo Scientific). Image capture and analysis, including densitometry, was performed with ImageLab software (Bio-Rad). Densitometry values were normalized to GAPDH for each condition. All western blot experiments were performed twice, and representative images are shown. Densitometry data is the composite of the two repeat experiments.

Statistical analyses

Data are presented as the mean ± standard deviation unless otherwise stated. Statistical significance was calculated via the Student's t-test or ANOVA as appropriate. Values of 0.05 were considered statistically significant. Analyses were performed using SPSS version 21 (IBM) and Prism 6 (GraphPad).

Results

Chemoresistant PDAC CAFs are more tumor-supportive than naïve CAFs

In order to begin to study the effect of cytotoxic chemotherapy on PDAC CAFs, gemcitabine resistant R-CAFs were generated from treatment naïve N-CAFs via 30 day incubation in 100nM gemcitabine. N-CAFs and R-CAFs were then compared for their ability to support tumor cell viability as well as migration and invasion. PDAC TCs demonstrated increased migration in R-CAF compared to N-CAF CM (MiaPaCa-2 p<0.0001, PANC-1 p<0.01) (Fig. 1A). Invasion was also increased for PANC-1 cells (p<0.0001) in R-CAF CM, however, this was not the case for MiaPaCa-2 cells (Fig. 1B). In addition to increased migration and invasion, TCs grown in R-CAF compared to N-CAF CM were more viable (Fig. 1C). Having demonstrated that R-CAFs support both TC growth and migration/invasion *in vitro*, we next assessed their effect *in vivo*. As seen in Fig. 1D, MiaPaCa-2 cells co-implanted with R-CAFs grew larger tumors than those co-implanted with N-CAFs.

R-CAFs upregulate multiple pro-inflammatory (SASP) cytokines

In order to elucidate the molecular mechanisms of the tumor-supportive phenotypes observed after gemcitabine treatment of CAFs, we performed a gene expression array analysis comparing R-CAFs and N-CAFs. There were a large number of molecular differences between the two cell types, with 994 transcripts comprising 738 genes demonstrating at least a 2-fold change in expression (Fig. 2A). Of note, multiple inflammatory cytokines were upregulated in R-CAFs (Fig. 2B). The gene expression changes in the array analysis in addition to the upregulation of several additional inflammatory mediators were validated by qRT-PCR (Fig. 2C). Cytokine array and IL-8 ELISA of R-CAF CM confirmed that the gene expression results correlate with secreted protein levels (Fig. 2D and E). Of note, this pattern of inflammatory cytokine expression has been observed after various senescence inducing stimuli and has been termed the senescence-associated secretory phenotype (SASP) (28). Importantly, while the SASP was originally described in the setting of senescence-inducing stimuli, its induction is independent of replicative arrest (28,29). To further investigate the contribution of a SASP-like response in R-CAFs, GSEA was applied to our data set. There was enrichment of 175 canonical pathways and biologic processes in R-CAFs, with several of the most enriched pathways involving cytokine signaling (Fig. 2F). GSEA was then applied to the identified pathways to assess for enrichment of a set of SASP genes previously described by Freund et al (26). SASP genes were significantly enriched (familywise enrichment ratio= 0.04) in R-CAFs compared to N-CAFs (Fig. 2F).

SASP induction occurs after short-duration treatment and is not gemcitabine specific

After observing SASP induction in R-CAFs, we sought to define the time-course of inflammatory cytokine upregulation. Upon treatment with gemcitabine, N-CAFs upregulated various SASP mediators beginning at 24h, with upregulation of the majority of SASP mediators seen in R-CAFs achieved by 48h (Fig. 3A). These kinetics indicate that the gene expression profile of R-CAFs is likely not the result of selection of a subpopulation of cells but rather a direct effect of gemcitabine on gene expression.

In addition to N-CAFs, a primary PDAC CAF line (CAF1) was treated with gemcitabine at various time points. Again, induction of multiple SASPs mediators was observed, although at later timepoints than in N-CAFs (Fig. 3B). To investigate whether the SASP response is gemcitabine specific or a more generalizable response to cytotoxic chemotherapeutic agents, N-CAFs were incubated with 5-FU for 48h. Treatment with 5-FU resulted in a pattern of SASP induction similar to that seen with gemcitabine (Fig. 3C).

SASP-induction is accompanied by activation of stress-associated MAPK signaling pathways

The major known upstream regulators of SASP induction are the DNA damage response (DDR) and P38 MAPK pathways (26). Therefore, we profiled N-CAFs, R-CAFs and N-CAFs treated with short-course gemcitabine for activation of DDR as well as P38 MAPK and JNK, a closely related stress-associated MAPK. After 48h of treatment with gemcitabine, N-CAFs showed some DDR activation as evidenced by increased phosphorylation of the DDR effector kinase Chk1. R-CAFs demonstrated a more modest increase in expression of p-Chk1 that did not reach statistical significance. Phosphorylation of Chk2, on the other hand, was not significantly different after chemotherapy treatment (Fig. 3D). Robust stress-associated MAPK signaling was seen in N-CAFs after gemcitabine treatment for 48h, with increased phosphorylation of P38 MAPK as well as JNK. Again, the response in R-CAFs was not as robust, but stress-associated MAPK activation was observed in these cells as well (Fig 3D).

Inhibition of stress-associated MAPK signaling in PDAC CAFs attenuates SASP induction

Having shown that both stress-associated MAPK and, to a lesser degree, DDR signaling are activated by gemcitabine treatment in CAFs, we screened a panel of inhibitors of various components of these signaling pathways for their ability to inhibit SASP induction. Inhibitors of stress-associated MAPK signaling were more effective than DDR inhibitors. The P38 inhibitor SB203580 and the JNK inhibitor SP600125 both inhibited cytokine production in N-CAFs induced by short-course GEM treatment. IL-6 and IL-8 expression were significantly decreased by both inhibitors. CXCL-1 expression was reduced after treatment with both inhibitors as well; however, this did not reach statistical significance. The PI3K related kinase (PI3K, ATM, ATR and DNA-PK) inhibitor NVP-BEZ235 and the ATM inhibitor KU55933 caused modest inhibition, while the ATR (VE-821) and Chk1/2 (AZD7762) inhibitors tested were not effective (Fig. 4A). Western blots confirmed target inhibition by SB203580 as evidenced by inhibition of HSP27 phosphorylation, a downstream target of P38 MAPK. Surprisingly, the effect of SP600125 on phosphorylation of c-JUN, a downstream JNK target, was minimal. Interestingly, SP600125 did inhibit p-HSP27, indicating that this inhibitor is likely not specific for JNK and also acts on P38 MAPK (Fig. 4B). In addition to N-CAFs, 3 primary CAF lines (CAF1-3) were treated with gemcitabine and the above listed inhibitors (Supplementary Fig. S3-4). While responses between different CAF lines were not completely consistent, inhibition of P38 MAPK or JNK tended to attenuate the gemcitabine-induced SASP. The DDR inhibitors NVP-BEZ235 and AZD7762 were more effective in primary CAFs than N-CAFs.

SASP inhibition attenuates the tumor-supportive phenotype of gemcitabine-treated CAFs

We next sought to investigate the phenotypic consequences of SASP inhibition in chemotherapy-treated CAFs. Based on the results of the drug screen, the P38 MAPK inhibitor SB203580 and the JNK inhibitor SP600125 were used to inhibit SASP induction. CM was generated from N-CAFs treated with or without gemcitabine and SB203580, SP600125, or DMSO control. As detailed in the methods, CM was generated after, not during, inhibitor treatment to avoid confounding results. TCs were assayed for migration, invasion and viability in the presence of CM. As expected, TCs (MiaPaCa-2 and PANC-1) exhibited increased migration and invasion in CM from gemcitabine-treated compared to untreated CAFs (p<0.0001). P38 MAPK or JNK inhibition during gemcitabine exposure significantly attenuated this response in both cell types, with the only exception being migration in MiaPaCa-2 cells. There was a dramatic impact on invasion in MiaPaCa-2 and PANC-1 cells, with P38 MAPK and JNK inhibition both resulting in near abrogation of the pro-invasive effect of gemcitabine treatment (p<0.0001, Fig. 5A). Consistent with previous results, TCs were more viable when grown in gemcitabine-treated CAF CM than untreated CM (MiaPaCa-2 and PANC-1 p<0.01). JNK inhibition attenuated the viability advantage produced by gemcitabine-treated CAF CM in MiaPaCa-2 (p<0.01) and PANC-1 (p<0.0001) cells (Fig. 5C). P38 MAPK inhibition had a significant effect on PANC-1 (p<0.01) but not MiaPaCa-2 viability (Fig. 5C). Overall, prevention of SASP induction by stress-associated MAPK inhibition significantly attenuated the tumor-supportive functions of gemcitabine-treated CAFs *in vitro*.

We next utilized our co-injection xenograft model to study the effect of stress-associated MAPK inhibition *in vivo*. N-CAFs were pre-treated for 48h with either DMSO control or gemcitabine with DMSO, SB203580, or SP600125 then co-implanted with TCs (MiaPaCa-2 or PANC-1). As expected, TCs implanted with gemcitabine pre-treated N-CAFs grew larger tumors than those implanted with untreated N-CAFs (p<0.0001, Fig. 6). The pro-tumorigenic effect of gemcitabine treatment was abrogated by P38 MAPK or JNK inhibition in MiaPaCa-2 tumors (p<0.0001, Fig. 6A) and attenuated by P38 MAPK inhibition in PANC-1 tumors (p<0.001, Fig. 6B).

Discussion

In this study, we demonstrate that chemotherapy-treated PDAC CAFs are more tumor-supportive than their naïve counterparts. Our results indicate that cytotoxic chemotherapy induces the upregulation of multiple inflammatory, SASP, mediators. Stress-associated MAPK signaling is identified as an important mediator of SASP induction in this setting. Blockade of SASP induction via inhibition of stress-associated MAPK signaling attenuates the tumor-supportive functions of chemotherapy treated CAFs.

The role of CAFs in promoting PDAC tumorigenesis as well as progression is well established (3-5). Among their many functions, PDAC CAFs are important contributors to a pro-inflammatory tumor microenvironment via their expression of multiple inflammatory mediators including IL-6, IL-8, and CXCL-1 at higher levels than normal fibroblasts (30-32). Inflammation is essential for the development of PDAC (4,33,34) as evidenced by the well-established link between chronic pancreatitis and cancer development (35,36).

Chronic inflammatory signaling has been implicated in the progression from low to high grade pancreatic intraepithelial neoplasia (PanIN), and eventually cancer (37,38). Furthermore, adult pancreatic cells are refractory to KRAS induced tumorigenesis in the absence of pancreatic inflammation (39). In addition to its role in PDAC development, inflammatory signaling is involved in the pathogenesis of PDAC growth and dissemination. Inflammatory cytokines such as IL-6 and IL-8 promote TC migration and invasion (40,41) as well as angiogenesis (41-43). Additionally, CAF-derived IL-6 contributes to evasion of immune surveillance by promoting myeloid-derived suppressor cell differentiation (9).

The induction of a pro-inflammatory SASP by various stimuli such as oncogene overexpression, radiation and cytotoxic chemotherapy has been implicated in cancer development and progression (26,44,45). The inflammatory factors that comprise the SASP are quite similar to those that are upregulated in CAFs compared to normal fibroblasts (30). It is interesting that we observe SASP induction following exposure to chemotherapy in PDAC CAFs given their known higher baseline expression of inflammatory mediators compared to normal fibroblasts. In prior studies, the major upstream pathways leading to SASP induction that have been indentified include DDR (29,46) and P38 MAPK (47,48) signaling. Our findings support the role of P38 MAPK as a SASP mediator in PDAC CAFs. Additionally, we provide new evidence that JNK, another stress-associated MAPK, can also contribute to SASP induction. Based on our chemical screen, DDR signaling appears to be a more important SASP mediator in primary as opposed to immortalized CAFs. This observation may be related to altered DDR signaling in p53 deficient immortalized cells. There was also heterogeneity observed in SASP expression and regulation between different primary CAFs, which may indicate differential responses to cytotoxic chemotherapy in CAFs from different patients.

Our finding of SASP induction in CAFs identifies a previously unknown detrimental effect of chemotherapy treatment on the tumor microenvironment in PDAC. The increased TC viability, migration and invasion that result from SASP induction oppose the positive effects of chemotherapy treatment. In our study, inhibition of the chemotherapy-induced SASP in PDAC CAFs attenuated their tumor-supportive phenotype. This raises the possibility that the SASP response in CAFs could be targeted to improve the efficacy of chemotherapy. Interestingly, despite their well-described protumorigenic functions, indiscriminate depletion of CAFs has been shown to accelerate PDAC progression (49,50), highlighting the need for targeted stromal therapies. The pro-inflammatory response to chemotherapy that our study identifies may represent a specific detrimental function of CAFs that could be targeted to improve therapy. We found stress-associated MAPK signaling pathways to be important drivers of the chemotherapy-induced SASP. Further studies will be necessary to assess the applicability of our results to actual human pancreatic cancer, including assessment of the impact of the pro-inflammatory response that we have observed on immune cells. We will also need to evaluate how stress-associated MAPK signaling can be targeted to achieve optimal synergy with cytotoxic chemotherapy. Additionally, refinement of our understanding of SASP regulation could lead to additional novel therapeutic targets.

In conclusion, we have identified a paradoxical effect of chemotherapy on the tumor microenvironment in PDAC. Chemotherapy-treated PDAC CAFs upregulate multiple pro-

inflammatory SASP mediators, leading to enhanced TC viability as well as migration and invasion. Inhibition of SASP induction can attenuate these tumor supportive functions. Signaling pathways controlling SASP induction after chemotherapy, including stress-associated MAPK, represent potential therapeutic targets that could improve the efficacy of current chemotherapeutic regimens.

Supplementary Material

Refer to Web version on PubMed Central for supplementary material.

Acknowledgments

References

1. Cancer Facts & Figures. American Cancer Society; Jun 16. 2014 2014<http://www.cancer.org/research/cancerfactsstatistics/cancerfactsfigures2014/index> [Accessed 2014 June 16, 2014]

2. Krejs GJ. Pancreatic cancer: epidemiology and risk factors. Dig Dis. 2010; 28(2):355–8. [PubMed: 20814212]

3. Feig C, Gopinathan A, Neesse A, Chan DS, Cook N, Tuveson DA. The pancreas cancer microenvironment. Clin Cancer Res. 2012; 18(16):4266–76. [PubMed: 22896693]

4. Apte MV, Wilson JS, Lugea A, Pandol SJ. A starring role for stellate cells in the pancreatic cancer microenvironment. Gastroenterology. 2013; 144(6):1210–9. [PubMed: 23622130]

5. Mahadevan D, Von Hoff DD. Tumor-stroma interactions in pancreatic ductal adenocarcinoma. Mol Cancer Ther. 2007; 6(4):1186–97. [PubMed: 17406031]

6. Vonlaufen A, Joshi S, Qu C, Phillips PA, Xu Z, Parker NR, et al. Pancreatic stellate cells: partners in crime with pancreatic cancer cells. Cancer Res. 2008; 68(7):2085–93. [PubMed: 18381413]

7. Hwang RF, Moore T, Arumugam T, Ramachandran V, Amos KD, Rivera A, et al. Cancer-associated stromal fibroblasts promote pancreatic tumor progression. Cancer Res. 2008; 68(3):918–26. [PubMed: 18245495]

8. Ikenaga N, Ohuchida K, Mizumoto K, Cui L, Kayashima T, Morimatsu K, et al. CD10+ pancreatic stellate cells enhance the progression of pancreatic cancer. Gastroenterology. 2010; 139(3):1041–51. 51.e1–8. [PubMed: 20685603]

9. Mace TA, Ameen Z, Collins A, Wojcik S, Mair M, Young GS, et al. Pancreatic cancer-associated stellate cells promote differentiation of myeloid-derived suppressor cells in a STAT3-dependent manner. Cancer Res. 2013; 73(10):3007–18. [PubMed: 23514705]

10. Kraman M, Bambrough PJ, Arnold JN, Roberts EW, Magiera L, Jones JO, et al. Suppression of antitumor immunity by stromal cells expressing fibroblast activation protein-alpha. Science. 2010; 330(6005):827–30. [PubMed: 21051638]

11. Tang D, Yuan Z, Xue X, Lu Z, Zhang Y, Wang H, et al. High expression of Galectin-1 in pancreatic stellate cells plays a role in the development and maintenance of an immunosuppressive microenvironment in pancreatic cancer. Int J Cancer. 2012; 130(10):2337–48. [PubMed: 21780106]

12. Miyamoto H, Murakami T, Tsuchida K, Sugino H, Miyake H, Tashiro S. Tumor-stroma interaction of human pancreatic cancer: acquired resistance to anticancer drugs and proliferation regulation is dependent on extracellular matrix proteins. Pancreas. 2004; 28(1):38–44. [PubMed: 14707728]

13. Muerkoster S, Wegehenkel K, Arlt A, Witt M, Sipos B, Kruse ML, et al. Tumor stroma interactions induce chemoresistance in pancreatic ductal carcinoma cells involving increased secretion and

paracrine effects of nitric oxide and interleukin-1beta. Cancer Res. 2004; 64(4):1331–7. [PubMed: 14973050]

14. Mantoni TS, Lunardi S, Al-Assar O, Masamune A, Brunner TB. Pancreatic stellate cells radioprotect pancreatic cancer cells through beta1-integrin signaling. Cancer Res. 2011; 71(10): 3453–8. [PubMed: 21558392]

15. Lunardi S, Muschel RJ, Brunner TB. The stromal compartments in pancreatic cancer: are there any therapeutic targets? Cancer Lett. 2014; 343(2):147–55. [PubMed: 24141189]

16. Neesse A, Michl P, Frese KK, Feig C, Cook N, Jacobetz MA, et al. Stromal biology and therapy in pancreatic cancer. Gut. 2011; 60(6):861–8. [PubMed: 20966025]

17. Olive KP, Jacobetz MA, Davidson CJ, Gopinathan A, McIntyre D, Honess D, et al. Inhibition of Hedgehog signaling enhances delivery of chemotherapy in a mouse model of pancreatic cancer. Science. 2009; 324(5933):1457–61. [PubMed: 19460966]

18. Provenzano PP, Cuevas C, Chang AE, Goel VK, Von Hoff DD, Hingorani SR. Enzymatic targeting of the stroma ablates physical barriers to treatment of pancreatic ductal adenocarcinoma. Cancer Cell. 2012; 21(3):418–29. [PubMed: 22439937]

19. Vaquero EC, Edderkaoui M, Nam KJ, Gukovsky I, Pandol SJ, Gukovskaya AS. Extracellular matrix proteins protect pancreatic cancer cells from death via mitochondrial and nonmitochondrial pathways. Gastroenterology. 2003; 125(4):1188–202. [PubMed: 14517801]

20. Lonardo E, Frias-Aldeguer J, Hermann PC, Heeschen C. Pancreatic stellate cells form a niche for cancer stem cells and promote their self-renewal and invasiveness. Cell Cycle. 2012; 11(7):1282–90. [PubMed: 22421149]

21. Hamada S, Masamune A, Takikawa T, Suzuki N, Kikuta K, Hirota M, et al. Pancreatic stellate cells enhance stem cell-like phenotypes in pancreatic cancer cells. Biochem Biophys Res Commun. 2012; 421(2):349–54. [PubMed: 22510406]

22. Sun Y, Campisi J, Higano C, Beer TM, Porter P, Coleman I, et al. Treatment-induced damage to the tumor microenvironment promotes prostate cancer therapy resistance through WNT16B. Nat Med. 2012; 18(9):1359–68. [PubMed: 22863786]

23. Rong G, Kang H, Wang Y, Hai T, Sun H. Candidate markers that associate with chemotherapy resistance in breast cancer through the study on Taxotere-induced damage to tumor microenvironment and gene expression profiling of carcinoma-associated fibroblasts (CAFs). PLoS One. 2013; 8(8):e70960. [PubMed: 23951052]

24. Bachem MG, Schunemann M, Ramadani M, Siech M, Beger H, Buck A, et al. Pancreatic carcinoma cells induce fibrosis by stimulating proliferation and matrix synthesis of stellate cells. Gastroenterology. 2005; 128(4):907–21. [PubMed: 15825074]

25. Kadera BE, Li L, Toste PA, Wu N, Adams C, Dawson DW, et al. MicroRNA-21 in pancreatic ductal adenocarcinoma tumor-associated fibroblasts promotes metastasis. PLoS One. 2013; 8(8):e71978. [PubMed: 23991015]

26. Freund A, Orjalo AV, Desprez PY, Campisi J. Inflammatory networks during cellular senescence: causes and consequences. Trends Mol Med. 2010; 16(5):238–46. [PubMed: 20444648]

27. Livak KJ, Schmittgen TD. Analysis of relative gene expression data using real-time quantitative PCR and the 2(−Delta Delta C(T)) Method. Methods. 2001; 25(4):402–8. [PubMed: 11846609]

28. Coppe JP, Patil CK, Rodier F, Sun Y, Munoz DP, Goldstein J, et al. Senescence-associated secretory phenotypes reveal cell-nonautonomous functions of oncogenic RAS and the p53 tumor suppressor. PLoS Biol. 2008; 6(12):2853–68. [PubMed: 19053174]

29. Rodier F, Coppe JP, Patil CK, Hoeijmakers WA, Munoz DP, Raza SR, et al. Persistent DNA damage signalling triggers senescence-associated inflammatory cytokine secretion. Nat Cell Biol. 2009; 11(8):973–9. [PubMed: 19597488]

30. Erez N, Truitt M, Olson P, Arron ST, Hanahan D. Cancer-Associated Fibroblasts Are Activated in Incipient Neoplasia to Orchestrate Tumor-Promoting Inflammation in an NF-kappaB-Dependent Manner. Cancer Cell. 2010; 17(2):135–47. [PubMed: 20138012]

31. Masamune A, Watanabe T, Kikuta K, Shimosegawa T. Roles of pancreatic stellate cells in pancreatic inflammation and fibrosis. Clin Gastroenterol Hepatol. 2009; 7(11 Suppl):S48–54. [PubMed: 19896099]

32. Andoh A, Takaya H, Saotome T, Shimada M, Hata K, Araki Y, et al. Cytokine regulation of chemokine (IL-8, MCP-1, and RANTES) gene expression in human pancreatic periacinar myofibroblasts. Gastroenterology. 2000; 119(1):211–9. [PubMed: 10889171]

33. Gukovsky I, Li N, Todoric J, Gukovskaya A, Karin M. Inflammation, autophagy, and obesity: common features in the pathogenesis of pancreatitis and pancreatic cancer. Gastroenterology. 2013; 144(6):1199–209.e4. [PubMed: 23622129]

34. Kolodecik T, Shugrue C, Ashat M, Thrower EC. Risk factors for pancreatic cancer: underlying mechanisms and potential targets. Front Physiol. 2013; 4:415. [PubMed: 24474939]

35. Lowenfels AB, Maisonneuve P, Cavallini G, Ammann RW, Lankisch PG, Andersen JR, et al. Pancreatitis and the risk of pancreatic cancer. International Pancreatitis Study Group. N Engl J Med. 1993; 328(20):1433–7. [PubMed: 8479461]

36. Pinho AV, Chantrill L, Rooman I. Chronic pancreatitis: a path to pancreatic cancer. Cancer Lett. 2014; 345(2):203–9. [PubMed: 23981573]

37. Fukuda A, Wang SC, Morris JPt, Folias AE, Liou A, Kim GE, et al. Stat3 and MMP7 contribute to pancreatic ductal adenocarcinoma initiation and progression. Cancer Cell. 2011; 19(4):441–55. [PubMed: 21481787]

38. Lesina M, Kurkowski MU, Ludes K, Rose-John S, Treiber M, Kloppel G, et al. Stat3/Socs3 activation by IL-6 transsignaling promotes progression of pancreatic intraepithelial neoplasia and development of pancreatic cancer. Cancer Cell. 2011; 19(4):456–69. [PubMed: 21481788]

39. Guerra C, Schuhmacher AJ, Canamero M, Grippo PJ, Verdaguer L, Perez-Gallego L, et al. Chronic pancreatitis is essential for induction of pancreatic ductal adenocarcinoma by K-Ras oncogenes in adult mice. Cancer Cell. 2007; 11(3):291–302. [PubMed: 17349585]

40. Huang C, Yang G, Jiang T, Huang K, Cao J, Qiu Z. Effects of IL-6 and AG490 on regulation of Stat3 signaling pathway and invasion of human pancreatic cancer cells in vitro. J Exp Clin Cancer Res. 2010; 29:51. [PubMed: 20482858]

41. Matsuo Y, Ochi N, Sawai H, Yasuda A, Takahashi H, Funahashi H, et al. CXCL8/IL-8 and CXCL12/SDF-1alpha co-operatively promote invasiveness and angiogenesis in pancreatic cancer. Int J Cancer. 2009; 124(4):853–61. [PubMed: 19035451]

42. Tang RF, Wang SX, Zhang FR, Peng L, Wang SX, Xiao Y, et al. Interleukin-1alpha, 6 regulate the secretion of vascular endothelial growth factor A, C in pancreatic cancer. Hepatobiliary Pancreat Dis Int. 2005; 4(3):460–3. [PubMed: 16109537]

43. Wente MN, Keane MP, Burdick MD, Friess H, Buchler MW, Ceyhan GO, et al. Blockade of the chemokine receptor CXCR2 inhibits pancreatic cancer cell-induced angiogenesis. Cancer Lett. 2006; 241(2):221–7. [PubMed: 16458421]

44. Hoare M, Narita M. Transmitting senescence to the cell neighbourhood. Nat Cell Biol. 2013; 15(8):887–9. [PubMed: 23907191]

45. Salama R, Sadaie M, Hoare M, Narita M. Cellular senescence and its effector programs. Genes Dev. 2014; 28(2):99–114. [PubMed: 24449267]

46. Pazolli E, Alspach E, Milczarek A, Prior J, Piwnica-Worms D, Stewart SA. Chromatin remodeling underlies the senescence-associated secretory phenotype of tumor stromal fibroblasts that supports cancer progression. Cancer Res. 2012; 72(9):2251–61. [PubMed: 22422937]

47. Freund A, Patil CK, Campisi J. p38MAPK is a novel DNA damage response-independent regulator of the senescence-associated secretory phenotype. Embo j. 2011; 30(8):1536–48. [PubMed: 21399611]

48. Alspach E, Flanagan KC, Luo X, Ruhland MK, Huang H, Pazolli E, et al. p38MAPK Plays a Crucial Role in Stromal-Mediated Tumorigenesis. Cancer Discov. 2014

49. Ozdemir BC, Pentcheva-Hoang T, Carstens JL, Zheng X, Wu CC, Simpson TR, et al. Depletion of carcinoma-associated fibroblasts and fibrosis induces immunosuppression and accelerates pancreas cancer with reduced survival. Cancer Cell. 2014; 25(6):719–34. [PubMed: 24856586]

50. Rhim AD, Oberstein PE, Thomas DH, Mirek ET, Palermo CF, Sastra SA, et al. Stromal elements act to restrain, rather than support, pancreatic ductal adenocarcinoma. Cancer Cell. 2014; 25(6): 735–47. [PubMed: 24856585]

Implications: Chemotherapy treatment of pancreatic cancer-associated fibroblasts results in a pro-inflammatory response driven by stress-associated MAPK signaling that enhances tumor cell growth and invasiveness.
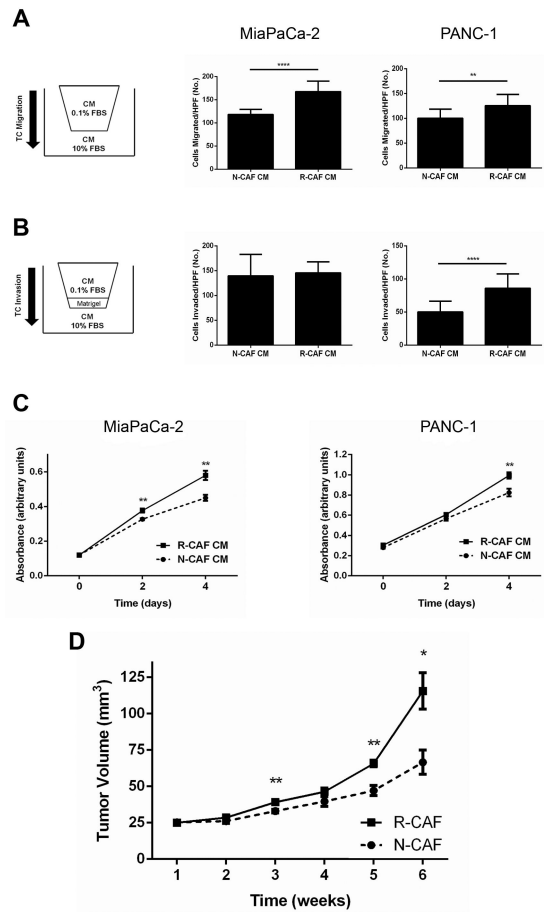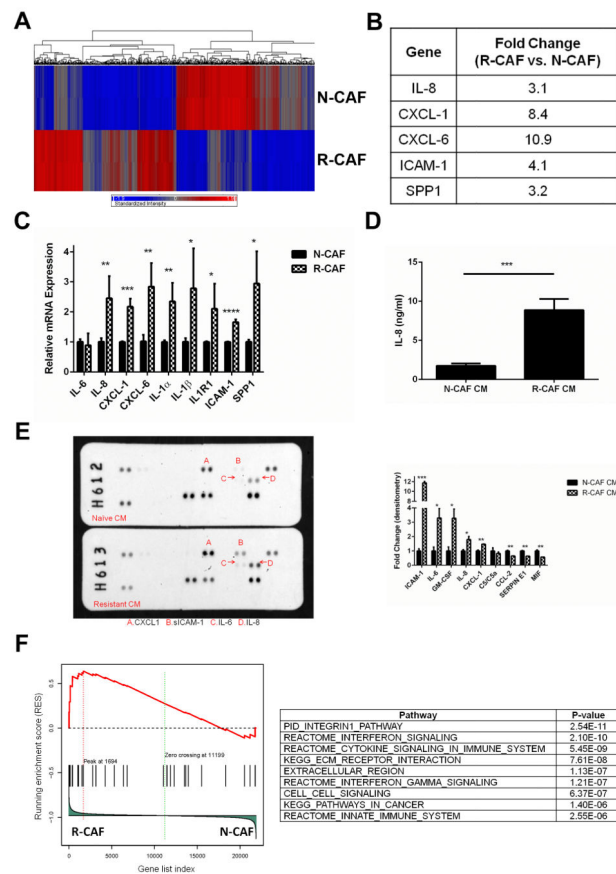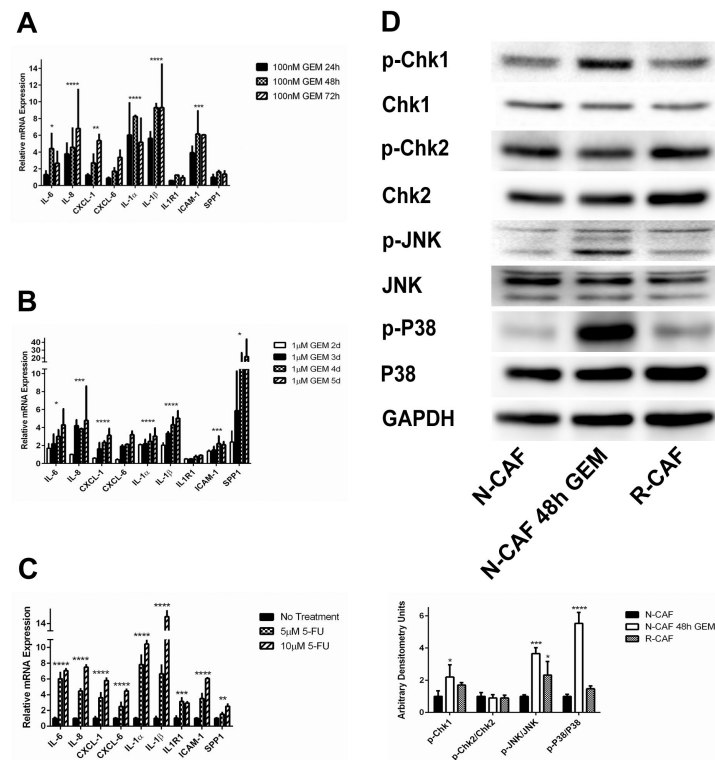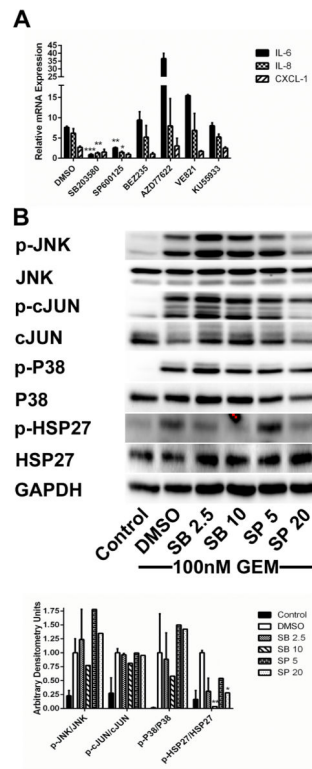
Figure 1.
Chemoresistant PDAC CAFs are more tumor-supportive than naïve CAFs. A, MiaPaCa-2
and PANC-1 cells were placed in uncoated transwell inserts with N-CAF or R-CAF CM for
18h and number of cells migrated per 20X field were quantified. B, MiaPaCa-2 and PANC-1
cells were placed in matrigel-coated transwell inserts under the same conditions as A for 28h
then quantified in the same fashion. C, Cell viability for MiaPaCa-2 and PANC-1 cells
grown in N-CAF or R-CAF CM supplemented with 1% FBS was quantified by MTT assay.
D, MiaPaCa-2 cells (1×10^5) were subcutaneously injected with either N-CAF or R-CAF
cells (3×10^5) in NSG mice (n=6 per group). Weekly CAF injections and tumor dimension
measurements were performed for the duration of the experiment. Data displayed are mean
volume +/− SEM. *p 0.05, **p 0.01, ****p 0.0001. For A-C, each experiment included
three biologic replicates.

Figure 2.
CAFs upregulate multiple inflammatory (SASP) cytokines in response to gemcitabine. A, heatmap demonstrating the multiple gene expression differences between N-CAFs and R-CAFs. 994 transcripts comprising 738 genes demonstrated at least a 2-fold difference in expression. B, summary of the inflammatory mediators upregulated in R-CAFs on gene expression array. C, qRT-PCR confirming the upregulation of various inflammatory mediators in R-CAFs. D, IL-8 ELISA comparing N-CAF and R-CAF CM. E, CM from N-CAFs and R-CAFs were subjected to antibody based cytokine array. A summary of the differential expression of the factors identified on the cytokine array is displayed below the blots. F, GSEA of the array data demonstrating enrichment of various pathways involving cytokine signaling in R-CAFs. The identified pathways were enriched for SASP genes (familywise enrichment ratio= 0.04). ***p 0.001. For C-E, data represent the composite of two separately performed experiments.

Figure 3.
SASP induction is seen with short duration treatment, is not gemcitabine specific and is accompanied by stress-associated MAPK activation. A, N-CAFs were incubated with 100nM GEM for the indicated times and qRT-PCR was used to quantify several SASP factors. B, The primary line CAF1 was incubated with 1μM GEM for the indicated times and qRT-PCR was used to quantify several SASP factors. C, N-CAFs were incubated with 5-FU (5μM or 10μM) for 48h, and SASP expression was quantified by qRT-PCR. D, N-CAFs treated with or without 100nM GEM for 48h and R-CAFs were assayed for activation of DDR and stress-associated MAPK signaling. Densitometry values are displayed below the blots. All values were normalized to GAPDH, and expression is displayed as the ratio of phospho- to total protein. *p 0.05, **p 0.01, ***p 0.001, ****p 0.0001 (ANOVA). For all experiments, data represent the composite of two separately performed experiments. The blots displayed in D are from one representative experiment.

Figure 4.
Inhibition of stress-associated MAPK signaling attenuates SASP expression in CAFs. A, N-CAFs were treated with 100nM GEM plus DMSO or the above listed small molecule inhibitors for 48h and SASP mediator expression was compared to untreated cells. Drug concentrations and targets: SB203580 10μM- P38 MAPK, SP600125 20μM- JNK, BEZ235 1μM- ATM/ATR/DNA-PK/PI3K/mTOR, AZD77622 200nM- Chk1/Chk2 VE821 2μM-ATR, KU55933 20μM- ATM. B, cell lysates from N-CAFs treated with 100nM GEM and DMSO, SB203580 or SP600125 at the indicated concentrations (μM) were blotted for P38 MAPK and JNK activation as well as their downstream targets, HSP27 and cJUN, respectively. Lysates from untreated N-CAFs were used as a control. Densitometry values are displayed below the blots. All values were normalized to GAPDH, and expression is displayed as the ratio of phospho- to total protein. For all experiments, data represent the composite of two separately performed experiments. The blots displayed in B are from one representative experiment.
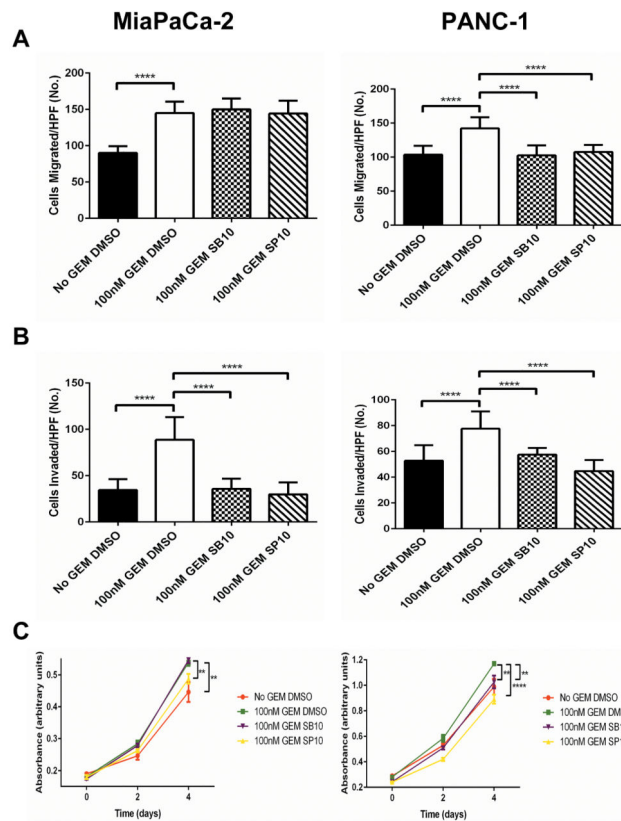
Figure 5.
SASP inhibition attenuates the tumor-supportive phenotype of gemcitabine-treated CAFs *in vitro*. A, MiaPaCa-2 and PANC-1 cells were assayed for migration by plating 1×10^5 cells in uncoated transwell inserts for 18h. Cells were placed in CM from N-CAFs treated with or without 100nM GEM in the presence of DMSO, 10μM SB203580 or 10μM SP600125. B, MiaPaCa-2 and PANC-1 cells were assayed for invasion by plating 1×10^5 cells in matrigel-coated transwell inserts for 28h. Cells were plated under the same conditions as in the migration assay. C, cell viability of MiaPaCa-2 and PANC-1 cells grown in CM from N-CAFs treated with or without 100nM GEM in the presence of DMSO, 10μM SB203580 or 10μM SP600125 was measured by MTT assay. CM for all of the above experiments was generated after, not during, inhibitor treatment to avoid the presence of inhibitor within the CM. **p 0.01, ****p 0.0001 (ANOVA). All experiments were performed with three biologic replicates.
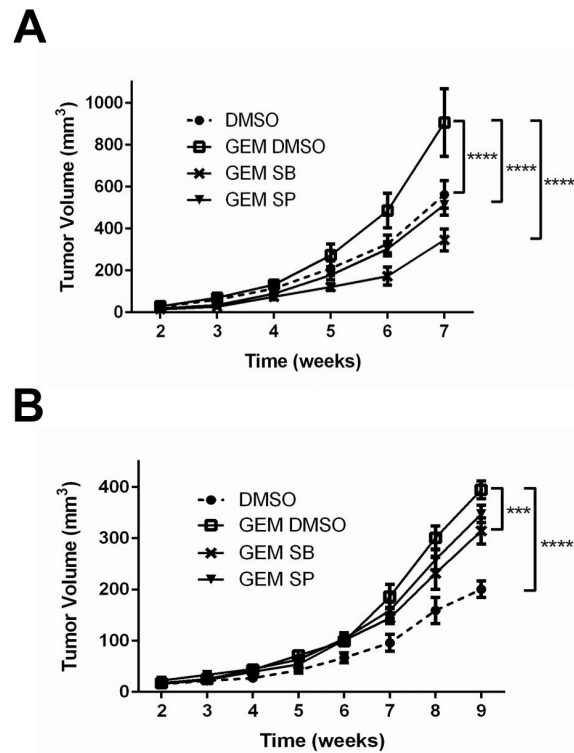
Figure 6.
SASP inhibition attenuates the tumor-supportive phenotype of gemcitabine-treated CAFs *in vivo*. A, MiaPaCa-2 cells (1×10^5) were subcutaneously injected with N-CAF cells (3×10^5) in NSG mice (n=6 per group). N-CAF cells were incubated for 48h prior to implantation with DMSO, gemcitabine+DMSO, gemcitabine+10μM SB203580, or gemcitabine+10μM SP600125. B, PANC-1 cells (1×10^5) were subcutaneously injected with N-CAF cells (3×10^5) in NSG mice (n=6 per group). N-CAF cells were pre-treated using the same conditions described above. Weekly CAF injections and tumor dimension measurements were performed for the duration of the experiment. Data displayed are mean volume +/− SEM. ***p 0.001, ****p 0.0001 (ANOVA).